

**Figure 5.** Stereopair views of the crystal packing patterns of triclinic **1** and **2**, viewed along [100] for **1** (top) and along [010] for **2**. **1** has two molecules per asymmetric unit, while **2** has only one.

4, a schematic pattern of the molecular packing shows how the *i*-related molecular stacks are interleaved in the structure of **1**. The red polymorph contains *i*-related molecules within a stack. In this structure, the Pd-Pd distance between neighboring molecules is 3.5 Å, and the molecular stack is parallel to the *c* axis (also the long axis of the red crystal plates). These packing pattern differences are seen in the stereopair views of the two structures in Figure 5.

On the basis of these structures and their relationship to the observed crystal expansion, we propose that the neighboring *i*-related molecular stacks in **1** slip together, as in a Martensitic transformation,<sup>9</sup> by moving along [011] in the direction of the long axis of the molecules. This would cause crystal fracture along the [010] planes, which is observed when thin crystals are heated. The crystal expansion occurs along the *c* axis (the needle axis) as expected from this mechanism. It remains a puzzle that the red color of **2** develops subsequent to rather than simultaneously with the expansion process. There are no unusually short intermolecular contacts in **2** that could account for the color change. This longer wavelength absorption may be due to the more extended conjugation in the planar conformation of **2**.<sup>10</sup> Since differential scanning calorimetry of the closely related molecules **3-6** (Chart I) reveals no solid-state rearrangements, it is clear that the solid-state changes observed for **1** are not due to any obvious property of the molecule itself but result from subtle packing properties which are not readily characterized. Anomalies such as these indicate that major advances in the field of solid-state chemistry are still needed in order to correlate molecular structure, crystal packing modes, and solid-state chemical and physical properties.

(9) (a) Smoluchowski, R.; Mayer, J. E.; Weyl, W. A., Eds. "Phase Transformations in Solids"; Wiley: New York, 1951: Chapter 1. (b) Private conversation with Prof. G. Wegner, who suggested the analogy between this transformation and a Martensitic transformation.

(10) Preliminary Raman data indicate that the 1375-cm<sup>-1</sup> N=N stretching band in solid **2** is resonance enhanced and, therefore, coupled to the long-wavelength transition. Following the arguments of Vrieze and co-workers, this suggests that the 480-nm absorption is, as proposed, connected with the diazo group.<sup>11,12</sup>

(11) VanBaar, J. F.; Vrieze, K.; Stufkens, D. J. J. *Organomet. Chem.* **1975**, *85*, 249.

(12) VanBaar, J. F.; Vrieze, K.; Stufkens, D. J. J. *Organomet. Chem.* **1975**, *97*, 461.

**Acknowledgment.** We thank Profs. R. D. Gillard and G. Wegner for their helpful discussions and suggestions and the staff of the 3M Analytical and Properties Research Laboratory (D. Markoe, W. Bahmet, G. Lillquist) for the DSC, powder diffraction, and Raman data.

**Registry No.** **1**, 84074-20-4; azobenzene, 103-33-3; palladium bis-(hexafluoroacetylacetonate), 65353-51-7.

**Supplementary Material Available:** Tables of atomic coordinates and temperature factors and Figures 1 and 2 (5 pages). Ordering information is given on any current masthead page.

### Design of Organic Metals Based on Tetramethyltetraselenafulvalene: Novel Structural Implications and Predictions

Jack M. Williams,\* Mark A. Beno, James C. Sullivan, Lisa M. Banovetz,<sup>†</sup> Julie M. Braam,<sup>†</sup> Gregory S. Blackman,<sup>†</sup> Clark D. Carlson,<sup>†</sup> Deena L. Greer,<sup>†</sup> and Diana M. Loesing<sup>†</sup>

Chemistry Division, Argonne National Laboratory  
Argonne, Illinois 60439

Received August 23, 1982

Presently at least six (TMTSF)<sub>2</sub>X metals, X = TaF<sub>6</sub><sup>-</sup>, SbF<sub>6</sub><sup>-</sup>, AsF<sub>6</sub><sup>-</sup>, PF<sub>6</sub><sup>-</sup>, ReO<sub>4</sub><sup>-</sup>, and ClO<sub>4</sub><sup>-</sup> where TMTSF = tetramethyltetraselenafulvalene, are reported superconductors.<sup>1</sup> All derivatives have superconducting (SC) *T*<sub>c</sub>'s ≈ 1 K, and except for (TMTSF)<sub>2</sub>ClO<sub>4</sub>, the only ambient-pressure<sup>2</sup> organic superconductor known, they all require an applied pressure of ~8-12 kbar in order to induce the SC state. Although all reported

<sup>†</sup> Research participation student under the auspices of the Division of Educational Programs, Argonne National Laboratory.

(1) For a general discussion of TMTSF metals see: *Mol. Cryst. Liq. Cryst.* **1982**, *79*, 1-359. TMTSF is Δ<sup>2,2'</sup>bi-4,5-dimethyl-1,3-diselenolyliidene.

(2) Bechgaard, K.; Carneiro, K.; Rasmussen, F. B.; Olsen, M.; Rindorf, G.; Jacobsen, C. S.; Pedersen, H. J.; Scott, J. C. *J. Am. Chem. Soc.* **1981**, *103*, 2440.

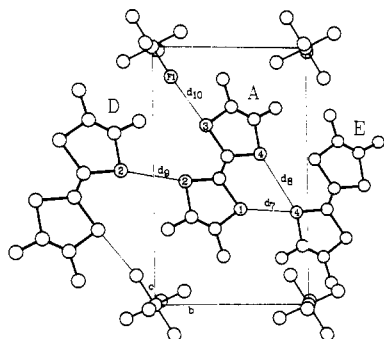


**Figure 1.** Short interstack Se-Se interactions in the extended sheet network,<sup>3,4</sup> characterized by the distances  $d_7$ ,  $d_8$ , and  $d_9$  ( $d < 4.0 \text{ \AA}$ ) in triclinic (TMTSF)<sub>2</sub>X metals. The shortest Se-Se distance in the temperature range  $T = 298 \rightarrow 125 \text{ K}$  is always  $d_9$ , and the longest is  $d_8$ . This Se-Se network expands or contracts in a systematic fashion depending on anion size.

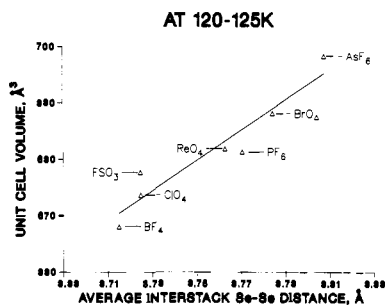


**Figure 2.** Plot of observed unit cell volume ( $V_c$ ) vs. the average<sup>5</sup> interstack Se-Se distance for various (TMTSF)<sub>2</sub>X metals at 125 K.

(TMTSF)<sub>2</sub>X salts are isostructural, they exhibit a wide variety of low-temperature ambient-pressure electrical properties ranging from semi- to superconducting, and yet the role of the anion is unclear.<sup>1</sup>

The 2:1 TMTSF salts discussed here are triclinic, space group  $P\bar{1}$ , and contain anions possessing octahedral or tetrahedral symmetry. The structures are characterized by (sometimes) slightly dimerized stacks (Table I, supplementary material) of nearly planar TMTSF molecules stacked along the crystal  $a$  axis. The TMTSF molecules also form infinite sheets extending in the  $ab$  plane (see Figure 1) which are separated by columns of anions. An important structural feature is the two-dimensional sheet network<sup>3,4</sup> of short inter- and intrachain Se-Se interactions having separation distances considerably less than the van der Waals radius sum ( $< 4.0 \text{ \AA}$ ). Finally, very anisotropic structural changes occur in these homoatomic Se atom separations as temperature is reduced ( $T = 298 \rightarrow 125 \text{ K}$ ), i.e., the interchain distances frequently decrease by as much as twice the intrachain (stack) distances.<sup>3,4</sup>

We have found anion- and temperature-induced changes in primary "structural" features that correlate with the pressure induced superconductivity in some derivatives, i.e., compared with (TMTSF)<sub>2</sub>ClO<sub>4</sub>, in which pressure is not required. The most obvious changes involve the short interchain Se-Se interactions ( $d_n < 4.0 \text{ \AA}$ ) occurring within the two-dimensional sheet network (see Figure 1). As the size of the anion is varied, there are systematic changes in both the observed unit cell volume,  $V_c$ , and the average interstack<sup>5</sup> Se-Se distances,  $d_{av}$ . In Figure 2 we have

plotted  $V_c$  vs.  $d_{av}$  for seven TMTSF derivatives using data derived from diffraction studies at 120–125 K.<sup>6,7</sup> The linear correlation is striking for three reasons:

(i) The minimum values of  $V_c$  and  $d_{av}$  cluster around that for ClO<sub>4</sub><sup>-</sup>, and inspection reveals that the ClO<sub>4</sub><sup>-</sup>, FSO<sub>3</sub><sup>-</sup>, and BF<sub>4</sub><sup>-</sup> salts are insignificantly different structurally at  $T = 125 \text{ K}$  ( $d_{av} = 3.715\text{--}3.725 \text{ \AA}$ ). This suggests the existence of very similar Se atom network geometry and low-temperature electrical properties if, in the absence of transitions such as anion ordering,<sup>8</sup> these structural trends continue down to  $T \sim 1 \text{ K}$ .

(ii) The incipient superconductors requiring pressure, which should decrease  $d_{av}$ , to induce the SC state all have  $d_{av}$  values above that of ClO<sub>4</sub><sup>-</sup> in Figure 2. This suggests that under an applied pressure the entire Se-Se sheet network shrinks in a predictable fashion until the structural architecture associated with the SC state is achieved.

(iii) It is now possible to predict the anion size required to produce a desired (TMTSF)<sub>2</sub>X metal with a tailored unit cell volume- $d_{av}$  combination because one may accurately predict unit cell volumes ( $V_{cp}$ ) on the basis of the anion chosen.<sup>9</sup> For any given monovalent octahedral or tetrahedral anion one may derive  $V_{cp}$  using the equations  $V_{cp} = 2.741 V + 645.00$  ( $T = 298 \text{ K}$ ) or  $V_{cp} = 1.743 V + 642.40$  ( $T = 125 \text{ K}$ ). With these equations ( $T = 125 \text{ K}$ ), the maximum deviation of  $V_{cp}$  vs.  $V_c$  for the six salts chosen<sup>9</sup> is 0.70% with the average deviation being 0.005%. For example, for ClO<sub>4</sub><sup>-</sup>,  $r_{Cl^{7+}} = 0.22 \text{ \AA}$  and  $r_{O^{2-}} = 1.21 \text{ \AA}$ , the calculated  $V_{cp} = 674.5 \text{ \AA}^3$ , and the observed  $V_c = 673.7 \text{ \AA}^3$  ( $T = 125 \text{ K}$ ). Similarly, for  $X = {}^{99}\text{TcO}_4^-$ , the first 2:1 TMTSF derivative to contain an internal source of radiation damage ( ${}^{99}\text{Tc}$ ,  $\beta^-$ ,  $2.12 \times 10^5$  years), the observed value<sup>12</sup> of  $V_c$  is  $686.1 \text{ \AA}^3$  and  $V_{cp} = 686.2 \text{ \AA}^3$  ( $T = 125 \text{ K}$ ).

Our results suggest that efforts aimed at the synthesis of new (TMTSF)<sub>2</sub>X derivatives, with possibly novel and enhanced electrical properties compared with (TMTSF)<sub>2</sub>ClO<sub>4</sub>, should center on use of previously untried anions with sizes comparable to ClO<sub>4</sub><sup>-</sup>, such as PO<sub>3</sub>F<sub>2</sub><sup>-</sup>, or on the preparation of anion alloys such as FSO<sub>3</sub><sup>-</sup>-ClO<sub>4</sub><sup>-</sup>, FSO<sub>3</sub><sup>-</sup>-BF<sub>4</sub><sup>-</sup>, BF<sub>4</sub><sup>-</sup>-ClO<sub>4</sub><sup>-</sup>, or BF<sub>4</sub><sup>-</sup>-ClO<sub>4</sub><sup>-</sup>-FSO<sub>3</sub><sup>-</sup>.<sup>13</sup> The theoretical significance of the correlations noted in this work are presented in the following paper.<sup>14</sup> The data analysis and conclusions presented here are applicable to any series of isostructural charge-transfer salts such as those of BEDT-TTF,<sup>15</sup> TMTTF,<sup>16</sup> etc.

**Acknowledgment.** Work supported by the U.S. Department Energy, Office of Basic Energy Sciences, Division of Materials

(6) Source references for the diffraction data used in this work are given in the supplementary material.

(7) A linear correlation of  $V_c$  vs.  $d_{av}$  is also obtained for the  $T = 298 \text{ K}$  data (Figure 1, supplementary data). Since we are primarily concerned with low-temperature properties only, the 125 K plot is given in the text.

(8) Jacobsen, C. S.; Pedersen, H. J.; Mortensen, K.; Rindorf, G.; Thorup, N.; Torrance, J.; Bechgaard, K. *J. Phys. C* **1982**, *15*, 2651 and references therein.

(9) Using effective ionic radii<sup>10</sup> and employing the methods of Shannon and Prewitt<sup>11</sup> for deriving effective multiautom ionic radii, one may predict unit cell volumes ( $V_{cp}$ ) in isostructural (TMTSF)<sub>2</sub>X salts. By plotting known  $V_c$ 's for six TMTSF salts ( $X = \text{PF}_6^-$ ,  $\text{ReO}_4^-$ ,  $\text{BrO}_4^-$ ,  $\text{ClO}_4^-$ ,  $\text{BF}_4^-$ , and  $\text{FSO}_3^-$ ) vs. the derived anionic volume  $V$ ,  $V = (r_i + 2r_o)^3$ , in arbitrary units, where  $r_i$  = ionic radius of inner ion and  $r_o$  = ionic radius of outer ion, one obtains linear least-squares fitted plots (Figures 2 ( $T = 298 \text{ K}$ ) and 3 ( $T = 125 \text{ K}$ ), supplementary data), from which  $V_{cp}$  may be calculated.

(10) Huheey, J. E. "Inorganic Chemistry—Principles of Structure and Reactivity", 2nd ed.; Harper and Row: New York, 1978; pp 71–74.

(11) Shannon, R. D.; Prewitt, C. T. *Acta Crystallogr., Sect. B* **1969**, *B25*, 925. Also see: Shannon, R. D. *Acta Crystallogr., Sect. A* **1976**, *A32*, 751.

(12) Williams, J. M.; Braam, J. M.; Beno, M. A.; Sullivan, J. C., work in progress.

(13) The observation of pressure-induced ( $p \approx 5 \text{ kbar}$ ) superconductivity in (TMTSF)<sub>2</sub>FSO<sub>3</sub> (P. M. Chaikin, submitted to *Phys. Rev. Lett.*) with a greatly increased  $T_c \approx 2.1 \text{ K}$  compared with (TMTSF)<sub>2</sub>ClO<sub>4</sub> strongly suggests that the ClO<sub>4</sub><sup>-</sup> Se-Se lattice framework may not be optimal for producing maximum  $T_c$  values.

(14) Whangbo, M.-H.; Williams, J. M.; Beno, M. A.; Dorfman, J. R. *J. Am. Chem. Soc.*, the following paper in this issue.

(15) Saito, G.; Enoki, T.; Toriumi, K.; Inokuchi, H. *Solid State Commun.* **1982**, *42*, 557.

(16) Liautaud, B.; Peytavin, S.; Brun, G.; Maurin, M. *J. Phys. (Orsay, Fr.)* **1982**, *43*, 1453.

(3) Williams, J. M.; Beno, M. A.; Appelman, E. H.; Wudl, F.; Aharon-Shalom, E.; Nalewajek, D. *Mol. Cryst. Liq. Cryst.* **1982**, *79*, 319.

(4) Beno, M. A.; Williams, J. M.; Lee, M. M.; Cowan, D. O. *Sol. State Commun.* **1982**, *44*, 1195.

(5) The average interstack Se-Se distance,  $d_{av} = (2d_7 + d_9)/3$ , is normalized according to the number of times the individual distance occurs in one unit cell. If the longest interstack Se-Se distance,  $d_8$ , is included in Figure 2, there are no significant changes, but the correlation coefficient is significantly reduced. A qualitatively similar, but significantly less pronounced, trend in average intrastack Se-Se distance vs.  $V_c$  is also observed.

Science, under Contract W-31-109-Eng-38.

Registry No. (TMTSF)<sub>2</sub>BF<sub>4</sub><sup>-</sup>, 73731-79-0; (TMTSF)<sub>2</sub>ClO<sub>4</sub><sup>-</sup>, 77273-54-2; (TMTSF)<sub>2</sub>FO<sub>3</sub>S<sup>-</sup>, 81259-79-2; (TMTSF)<sub>2</sub>ReO<sub>4</sub><sup>-</sup>, 80531-49-3; (TMTSF)<sub>2</sub>PF<sub>6</sub><sup>-</sup>, 73261-24-2; (TMTSF)<sub>2</sub>BrO<sub>4</sub><sup>-</sup>, 81259-81-6; (TMTSF)<sub>2</sub>AsF<sub>6</sub><sup>-</sup>, 73731-75-6.

**Supplementary Material Available:** Full structural details for the (TMTSF)<sub>2</sub>X salts reported herein including source and reference diffraction data used in this work, plane dimerization distances ( $D_1$  and  $D_2$ ), interstack Se-Se contact distances ( $d_7$ ,  $d_8$ , and  $d_9$ ), and plots of known unit cell volumes versus derived ionic volumes ( $T = 298$  and  $125$  K) (6 pages). Ordering information is given on any current masthead page.

### Characterization of the Interchain Se...Se Interaction in (TMTSF)<sub>2</sub>X by Band Electronic Structure

Myung-Hwan Whangbo,<sup>\*1a</sup> Jack M. Williams,<sup>\*1b</sup>  
Mark A. Beno,<sup>1b</sup> and Jay R. Dorfman<sup>1a</sup>

Department of Chemistry, North Carolina State University  
Raleigh, North Carolina 27650  
Chemistry Division, Argonne National Laboratory  
Argonne, Illinois 60439  
Received August 23, 1982

Crystal structures of (TMTSF)<sub>2</sub>X salts exhibit a systematic decrease in the interchain Se...Se separations upon decreasing the unit cell volume or upon lowering temperature.<sup>2</sup> Such structural changes hold important information concerning how the interchain Se...Se separation is related to the magnitude of the interchain Se...Se interactions. To explore this relationship, we examined the electronic structures of (TMTSF)<sub>2</sub>X ( $X^- = \text{AsF}_6^-, \text{BF}_4^-, \text{BrO}_4^-, \text{ClO}_4^-, \text{FSO}_3^-, \text{H}_2\text{F}_3^-, \text{PF}_6^-, \text{and ReO}_4^-$ ) by performing the tight-binding band calculations based upon the extended Hückel method.<sup>3</sup> Our calculations on all (TMTSF)<sub>2</sub>X compounds employed their crystal structures determined at 298 K and at 120-125 K.<sup>2,4</sup> Actual band-structure calculations for each (TMTSF)<sub>2</sub>X salt were carried out on a two-dimensional sheet of TSF molecules,<sup>5</sup> as reported elsewhere.<sup>6,7</sup>

<sup>†</sup> Camille and Henry Dreyfus Teacher-Scholar (1980-1985).

<sup>\*</sup> Present Address: Department of Chemistry, Harvard University, Cambridge, MA 02138.

(1) (a) North Carolina State University; (b) Argonne National Laboratory.

(2) Williams, J. M.; Beno, M. A.; Banovetz, L. M.; Braam, J. M.; Blackman, G. S.; Carlson, C. D.; Greer, D. L.; Loesing, D. M. *J. Am. Chem. Soc.*, preceding paper in this issue.

(3) (a) Whangbo, M.-H.; Hoffmann, R. *J. Am. Chem. Soc.* **1978**, *100*, 6093. (b) Whangbo, M.-H.; Hoffmann, R.; Woodward, R. B. *Proc. R. Soc. London, Ser. A* **1979**, *366*, 23.

(4) The crystal structures of (TMTSF)<sub>2</sub>X used in our study were our own work and also taken from the following: (a) Thorp, N.; Rindorf, G.; Soling, H.; Bechgaard, K. *Acta Crystallogr. Sect. B* **1981**, *37B*, 1236. (b) Bechgaard, K.; Carneiro, K.; Rasmussen, F. B.; Olsen, M.; Rindorf, G.; Jacobsen, C. S.; Pedersen, H. J.; Scott, J. C. *J. Am. Chem. Soc.* **1981**, *103*, 2440. (c) Wudl, F. *Ibid.* **1981**, *103*, 7065. (d) Williams, J. M.; Beno, M. A.; Appelman, E. H.; Capriotti, J. M.; Wudl, F.; Aharon-Shalom, E.; Nalewajek, D. *Mol. Cryst. Liq. Cryst.* **1982**, *79*, 319. (e) Beno, M. A.; Williams, J. M.; Lee, M. M.; Cowan, D. O. *Solid State Commun.* **1982**, *44*, 1195. (f) Beno, M. A.; Blackman, G. S.; Williams, J. M.; Bechgaard, K. *Inorg. Chem.* **1982**, *21*, 3860. (g) Rindorf, G.; Soling, H.; Thorp, N., submitted for publication in *Acta Crystallogr., Sect. B*.

(5) The acronyms TMTSF and TSF refer to tetramethyl-tetraselenafulvalene and tetraselenafulvalene, respectively.

(6) Whangbo, M.-H.; Walsh, W. M., Jr.; Haddon, R. C.; Wudl, F. *Solid State Commun.* **1982**, *43*, 637.

(7) The  $H_{\mu\nu}$  value for Se 4p orbital was taken as -12.7 eV instead of -14.4 eV,<sup>8</sup> since the former reproduces the semimetallic property of TiSe<sub>2</sub>.<sup>8</sup> However, these two parameters lead to band structures very similar in nature. The  $H_{\mu\nu}$  value for Se 4d orbital was taken as -7.0 eV,<sup>6</sup> which provides a one-electron band structure consistent with the Shubnikov-de Haas data on (TMTSF)<sub>2</sub>PF<sub>6</sub>.<sup>6,9,10</sup> Calculations with and without Se 4d orbitals exhibit the same trends for the qualitative aspects of the interchain Se...Se interaction, although the intrachain and the interchain bandwidths are enhanced upon including Se 4d orbitals.<sup>6</sup> Thus we report only those results obtained without Se 4d orbitals, which should be regarded as a lower limit.<sup>11</sup>

(8) Ragavachari, K., private communication.

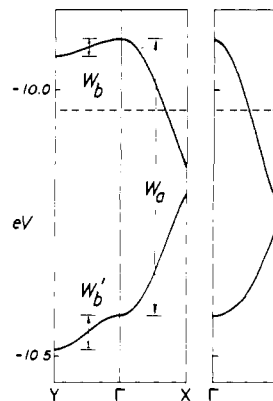


Figure 1. Band structure of a two-dimensional sheet of TSF molecules. The symbols  $\Gamma$ ,  $X$ ,  $Y$ , and  $V$  refer to the points in the Brillouin zone,<sup>6</sup> whose coordinates are expressed in fractions of the reciprocal vectors  $a^*$  and  $b^*$  as follows:  $\Gamma = (0.0, 0.0)$ ,  $X = (0.5, 0.0)$ ,  $Y = (0.0, 0.5)$ , and  $V = (0.5, 0.5)$ . The Fermi level is indicated by the dashed line.

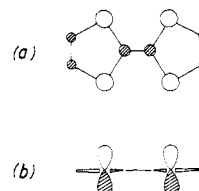
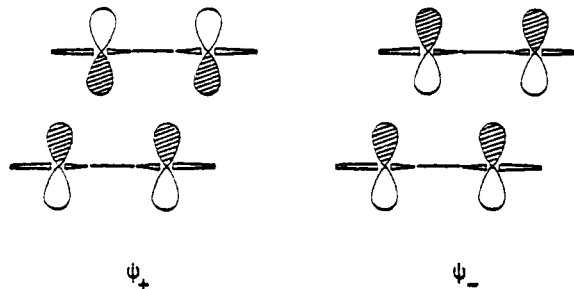


Figure 2. Schematic representations of the HOMO of a TSF molecule. The Se 4p and C 2p orbitals are projected onto the molecular plane in a. The side view of the HOMO is given in b, where only the Se 4p orbitals are shown for simplicity.

The valence band (i.e., the highest occupied band) of every (TMTSF)<sub>2</sub>X has the characteristic feature shown in Figure 1 for (TMTSF)<sub>2</sub>PF<sub>6</sub> at 125 K. That is, the valence band consists of two overlapping bands.<sup>6</sup> With the formal oxidation of (TMTSF)<sub>2</sub><sup>+</sup> per unit cell, the valence band is one-quarter-empty because of the half-empty upper band and the completely filled lower band. The HOMO of each TSF molecule has large coefficients on Se 4p orbitals, as schematically shown in Figure 2. Two such HOMO's in each unit cell of (TMTSF)<sub>2</sub>X interact to form the in-phase and the out-of-phase combinations ( $\psi_+$  and  $\psi_-$ , respec-



tively). It is these orbitals  $\psi_+$  and  $\psi_-$  that lead to the lower and the upper bands of Figure 1, respectively. The valence band of (TMTSF)<sub>2</sub>X may be characterized by three calculated parameters, i.e., the combined width  $W_a$  of the two overlapping bands along the chain direction ( $\Gamma \rightarrow X$ ), the width  $W_b$  of the upper band along the interchain direction ( $\Gamma \rightarrow Y$ ), and the width  $W_b'$  of the lower band along the interchain direction.

The magnitude of interaction between neighboring unit cells in a certain direction is proportional to the width of the resulting band in that direction. Therefore, both  $W_b$  and  $W_b'$  are associated

(9) Kwak, J. F.; Schirber, J. E.; Greene, R. L.; Engler, E. M. *Phys. Rev. Lett.* **1981**, *46*, 1296.

(10) Horowitz, B.; Gutfreund, H.; Weger, M. *Solid State Commun.* **1981**, *39*, 541; *Mol. Cryst. Liq. Cryst.* **1982**, *79*, 155.

(11) (a) Grant, P. M. *Phys. Rev. B: Condens. Matter* **1982**, *26*, 6888. (b) Jacobsen, J. C.; Tanner, D. B.; Bechgaard, K. *Phys. Rev. Lett.* **1981**, *46*, 1142; *Mol. Cryst. Liq. Cryst.* **1982**, *79*, 25.